Chemical Engineering Journal 157 (2010) 45–51

Contents lists available at ScienceDirect

Chemical Engineering Journal

journal homepage: www.elsevier.com/locate/cej

Synthesis, characterization, and photocatalytic application of novel TiO_2 nanoparticles

M. Hussain, R. Ceccarelli, D.L. Marchisio, D. Fino, N. Russo*, F. Geobaldo

Department of Materials Science and Chemical Engineering, Politecnico di Torino, Corso Duca degli Abruzzi 24, 10129 Torino, Italy

ARTICLE INFO

Article history:
Received 17 July 2009
Received in revised form 15 October 2009
Accepted 16 October 2009

Keywords:
TiO_2
Nanoparticles
Sol–gel
Ethylene
Oxidation
Photocatalysis

ABSTRACT

Novel TiO_2 nanoparticles (TNP) having a high specific surface area were successfully synthesized in a vortex reactor by sol–gel process with optimized operating parameters. These 10–20 nm TNP were characterized and compared with TiO_2 synthesized by solution combustion (TSC) method and commercially available TiO_2 (degussa P25 and anatase by Aldrich). Characterization was performed by X-ray diffraction spectroscopy (XRD), specific surface area analysis, energy dispersive X-ray spectroscopy (EDX), scanning electron microscopy (SEM), diffuse reflectance ultraviolet–visible spectroscopy (DR/UV–vis), and Fourier transformed-infrared spectroscopy (FT-IR). TNP showed comparatively smaller size with little porosity between them, good crystalline anatase with small rutile phase, higher BET surface area, confined band gap energy, and higher OH groups. Photocatalytic oxidation of ethylene (a naturally occurring gas produced by plant tissues, engine exhausts, and plant and fungi metabolism) has been investigated at ambient temperature in an ad hoc designed pyrex glass photocatalytic reactor, by using these TNP and compared with TSC, and commercial TiO_2. Higher photocatalytic conversion of ethylene was observed for TNP compared to TSC and commercial TiO_2. Mixed phase of TN with high surface area might induce the adsorption of ethylene pollutant and water with generation of OH groups (oxidizing agent) on the surface of TNP leading to higher photocatalytic activity.

1. Introduction

The first discovery of the photochemical hydrolysis of water by Fujishima and Honda [1] has opened the field of diverse applications of titania in areas such as photovoltaics [2], self-cleaning coatings [3], photocatalysis [4], and electrochronic display devices [5]. Photocatalysts are solids that can promote reactions in the presence of light without being consumed [6].

TiO_2 is an ideal photocatalyst in several ways. It is relatively cheap, highly stable from a chemical viewpoint, and easily available. Moreover, its photogenerated holes are highly oxidizing, and the photogenerated electrons are reducing enough to produce superoxide from dioxygen. It promotes ambient temperature oxidation of the major classes of indoor air pollutants, and does not need any chemical additives [7–9]. Air pollution is considered worldwide a serious problem. Volatile organic compounds (VOCs) the main part of the air pollution are from the indoor as well as external sources. Conventionally, VOC pollutants are removed by air purifiers that employ filters to remove particulate matters or use sorption materials (e.g. granular activated carbon) to adsorb the pollutants. These techniques only transfer the contaminants to another phase rather than eliminating them. Hence, additional disposal or handling steps are needed. Photocatalytic oxidation (PCO) of VOCs is a promising alternative technology for air purification. It has been demonstrated that organics can be oxidized to carbon dioxide, water and simple mineral acids at low temperature on TiO_2 catalysts in the presence of UV or near-UV illumination [10–19].

Most of the studies have shown that the photocatalytic activity of titanium dioxide is greatly influenced by the crystalline form, although controversial results are reported in the literature. For example, some authors state that anatase works better than rutile [17,20], others found the best photocatalytic activity for rutile [21–23], and some others detected synergistic effects in the photocatalytic activity for anatase–rutile mixed phases [24–26]. Besides, recently it was demonstrated that photoactivity in organics degradation depends on the phase composition and on the oxidizing agent [27]. Moreover the ability of titanium dioxide particles to degrade organic compounds depends also on the size of the particles, since small particles offer larger specific surface areas [28].

Many processes can be employed for the production of titanium dioxide particles, such as flame aerosol synthesis [29], hydrothermal synthesis [30], and sol–gel synthesis [31]. Flame aerosol synthesis presents the main advantage of being easily scalable to the industrial level, but shows all the disadvantages of high temperature synthesis. Hydrothermal synthesis is instead particularly interesting for it directly produces a crystalline powder, without the

* Corresponding author. Tel.: +39 011 0904710; fax: +39 011 5644699.
E-mail address: nunzio.russo@polito.it (N. Russo).

1385-8947/$ – see front matter © 2009 Elsevier B.V. All rights reserved.
doi:10.1016/j.cej.2009.10.043

need of a final calcination step, which is necessary in the sol–gel process. However, the lack of knowledge of the chemical equilibria of the species in solution and of the kinetics of nucleation and growth of the different phases makes it difficult to control the overall process. Therefore, the sol–gel process is at the moment the most common and promising one at a lab scale. Although the sol–gel process has been known almost for a century and some of the most important aspects have been cleared, there exists room for improvement for individuating synthesis conditions that result in a powder with improved properties, when compared with the commercial products available at the moment. Furthermore, upscaling the process from the laboratory to the industrial scale is still a complex problem of difficult solution. Mixing plays indeed a big role but its effects are usually underestimated, as proven by the qualitative statements (e.g. add drop wise or mix vigorously) generally used to define ideal mixing conditions.

In our previous studies of synthesis of TiO_2 nanoparticles [32,33], we have investigated quantitatively the effect of mixing and other operating parameters. This synthesis study was done on small scale, where the reported results clearly show that mixing plays a key role. The use of adaptable mixing devices, such as the one described, allows tuning the mixing rate in order to obtain the desired particle size and morphology.

In the present work, we particularly focused on the synthesis of novel TiO_2 nanoparticles (TNP) on large scale by controlling the optimized operating conditions and using a special passive mixer, i.e. a vortex reactor (VR). We made an attempt to get TNP with high surface area and mixed crystalline phase with more anatase and small amounts rutile. Because of the mentioned synergistic effect, the mixed phases are expected to be more attractive for gas-phase photocatalytic application of VOC in the presence of oxygen [24]. Ethylene was chosen as a probe reactant for the application of TNP. It is generated by engines; biomass fermentators; pyrolysis of hydrocarbons; fruit ripening; and plants biosynthesis. Besides, it is also the parent compound of more widespread class of VOCs of environmental concern (e.g. trichloroethylene and tetrachloroethylene). Some researchers [10–13] have already focused on the ethylene degradation by catalysts at relatively higher temperature than the ambient temperature. However, in this study we have focused on the use of the synthesized TNP photocatalyst for ethylene degradation at ambient temperature. A new fabricated photocatalytic reaction system with pyrex glass reactor is used. Comparison was accomplished with TiO_2 synthesized by solution combustion method (TSC) or commercial TiO_2. Characterization was performed by X-ray diffraction spectroscopy (XRD), Brunauer–Emmet–Teller (BET) analysis, energy dispersive X-ray spectroscopy (EDX), field emission scanning electron microscopy (FE-SEM), diffuse reflectance ultraviolet–visible spectroscopy (DR/UV–vis), and Fourier transformed-infrared spectroscopy (FT-IR).

2. Experimental

2.1. Synthesis of TiO_2

TNP were synthesized on large scale (2 L gel) by controlling the optimized operating parameters using the VR shown in Fig. 1, and by adopting the small scale (200 mL gel) synthesis procedure [32,33]. Titanium tetra-isopropoxide (TTIP: Sigma–Aldrich) was used as a precursor in this work, because of its very rapid hydrolysis kinetics. Two solutions of TTIP in isopropyl alcohol and of water (Milli-Q) in isopropyl alcohol were prepared separately under nitrogen flux to control the alkoxide reactivity with humidity. Hydrochloric acid (HCl: Sigma–Aldrich) was added to the second solution as a hydrolysis catalyst and deagglomeration agent. TTIP/isopropanol concentration was taken equal to 1 M to

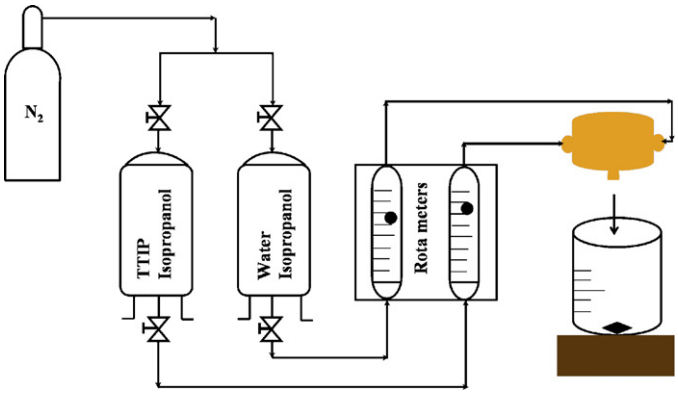

Fig. 1. TNP (sol–gel method) synthesis set-up.

get the maximum TiO_2 (1 M), whereas the water and hydrochloric acid concentrations were chosen in order to result in a water to precursor ratio, $W = [H_2O]/[TTIP]$, equal to four, and acid to precursor ratio, $H = [H^+]/[TTIP]$, equal to 0.5. The two solutions of TTIP and water in isopropyl alcohol were stored in two identical vessels, then pressurized at 2 bars with analytical grade nitrogen, and eventually fed and mixed in the VR. The inlet flow rates were kept equal to 100 mL/min by using two rotameters. This inlet flow rate guarantees very fast mixing, thus inducing the formation of very fine particle. Equal volumes of reactant solutions (i.e. 1 L) were mixed at equal flow rates at 28 °C and then for both configurations the solutions exiting the VR were collected in a beaker thermostated at 28 °C and gently stirred. The TTIP conversion into TiO_2 through hydrolysis and condensation can be summarized into the following global chemical reaction:

$$Ti(OC_3H_7)_4 + 4H_2O \rightarrow TiO_2 + 2H_2O + 4C_3H_7OH$$

As it is well known that a very fast chemical reaction characterized by an equilibrium completely shifted toward the products, as TiO_2 is a thermodynamically very stable substance, thus resulting in almost 100% yield.

The reaction product (i.e. gel) was then dried in three different ways; dried by rotavapor, directly in oven, and in oven after filtration. The resulting dried powders were eventually calcined at 400 °C for 3 h.

TSC was synthesized by following the procedure reported in [34] but with modified precursors and ratios. Particularly TTIP was used as precursor, glycine/urea as fuel, under stochiometric as well as non-stochiometric ratios, and 400/500 °C as combustion temperature. After combustion reaction, the samples were followed for calcinations at 400 °C for 3 h. Different commercial TiO_2 were purchased from Sigma–Aldrich and Aerosil to make comparison.

2.2. Characterization

In order to determine the different polymorphs, XRD patterns were recorded on a X'Pert Phillips diffractomer using Cu Kα radiation, in the following conditions: range = (10–90°) 2θ; step size $2\theta = 0.02°$. The BET surface area measurement and pore size analysis were carried out on powders previously outgassed at 150 °C, by N_2 sorption at 77 K on a Quantachrome Autosorbe 1C instrument. FE-SEM pictures were collected on a high-resolution FE-SEM instrument (LEO 1525) equipped with a Gemini field emission column to see the particle morphology; with the same instrument, elemental composition was checked by EDX analysis.

Information about the nature of OH groups was obtained with a FT-IR spectroscopy. Powders were pressed into thin, self-supporting wafers. Spectra were collected, at a resolution of 2 cm^{-1}

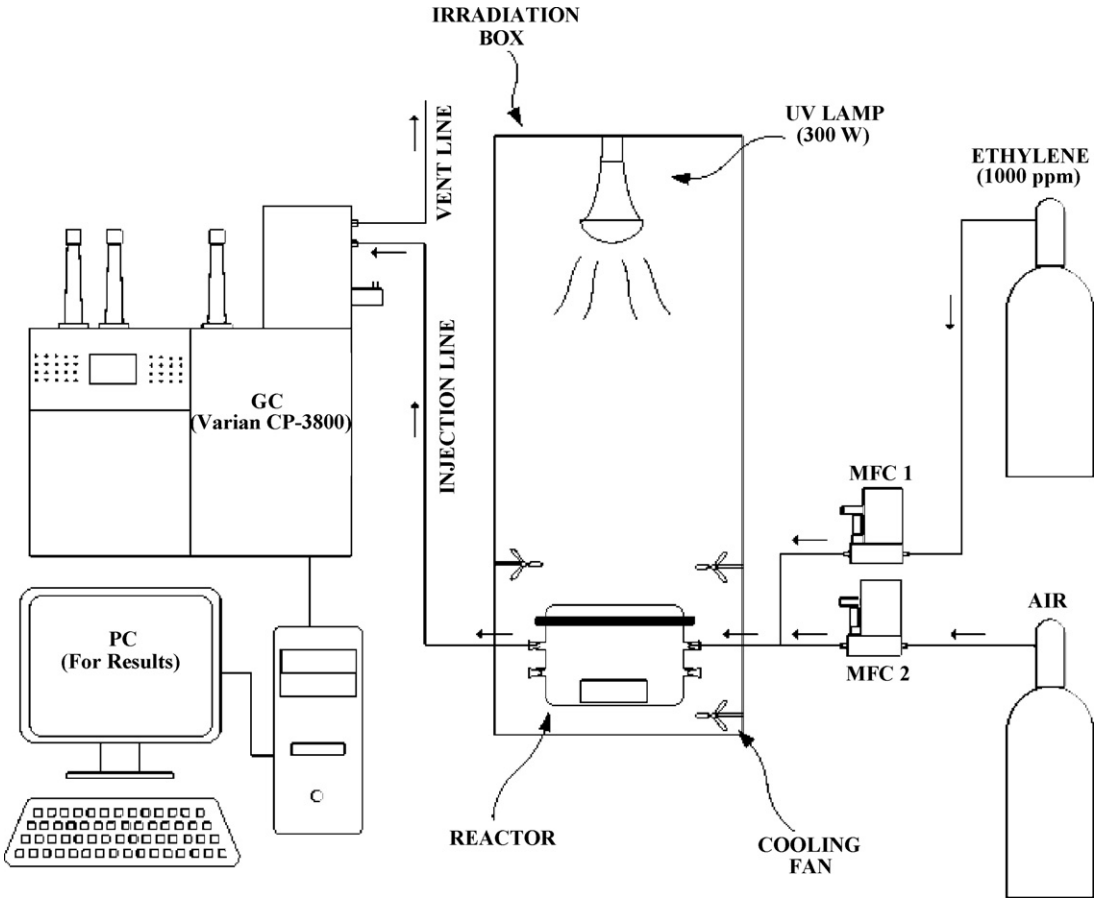

Fig. 2. Photocatalysis reaction experimental setup.

on a Perkin Elmer FT-IR spectrophotometer equipped with a MCT detector.

DR/UV–vis was done by a UV–vis double beam spectrophotometer Varian Cary 500, equipped with an integrating sphere. For background subtraction, the reference was Spectralon® and spectra were collected in 200–600 nm regions with a resolution of 2 nm. The measuring set-up permits the analysis of diffuse radiation, excluded the specular one.

2.3. Ethylene photocatalytic reaction

All tests of ethylene photocatalytic degradation were performed in a pyrex glass reactor with total volume of 2000 cm^3. A schematic of the experimental setup is depicted in Fig. 2, that includes the pyrex glass reactor (transparent to UV light), connectors, mass flow controllers (MFC, Bronkhorst high tech), UV lamp (Osram ultra vitalux, 300 W), gas cylinders (1000 ppm ethylene, air), and gas chromatograph (Varian CP-3800) equipped with capillary column (CP7381, fused silica) and flame ionization detector (FID) with a patented ceramic flame tip for ultimate peak shape and sensitivity, used for the product gas analysis.

1 g calcined TiO_2 sample was dispersed inside the pyrex glass reactor. 100 ppm ethylene was continuously flushed in the reactor with the help of MFC at constant flow rate of 50 mL/min. After achieving equilibrium in the peak intensity, UV light was turned on, reaction products were analyzed by GC, and ethylene conversion was calculated.

We repeated our experiments and the results were reproducible. Therefore, we safely state that the errors are quite limited and can be neglected.

3. Results and discussion

3.1. Characterization and comparison of TiO_2 samples

TNP were dried in three different commercial process leading easy ways to find the optimized one. After drying and before calcination the powder is mainly amorphous and no distinct peak is found, as shown in Fig. 3(a). However, after calcination at 400 °C for 3 h the main crystalline form was anatase (denoted as "A") and minor part in rutile (denoted as "R") (Fig. 3(a)). The optimal drying condition was found by drying in rotavapor, resulting in an anatase to rutile ratio of 80:20. Details and comparison with the other drying conditions are reported in Table 1. For most photocatalytic reaction systems, it is generally accepted that anatase demonstrates a higher activity than rutile and this enhancement in photoactivity has been ascribed to the Fermi level

Table 1
BET surface area and crystalline phases of different TiO_2.

Sample	S_{BET} (m^2/g)	Anatase:rutile (%)
TNP (rotavapor dried and calcined)	151	80:20
TNP (filtered, dried and calcined)	130	71:29
TNP (oven dried and calcined)	121	69:31
TSC (glycine, 400 °C, 1:1)	85	55:45
TSC (glycine, 500 °C, 1:1)	90	60:40
TSC (urea, 500 °C, 1:3)	108	61:39
TSC (urea, 500 °C, 1:1)	65	58:42
TiO_2 commercial (Aldrich, technical)	15	80:20
TiO_2 commercial (Aldrich, anatase)	10	100:0
TiO_2 commercial (degussa P25)	53	70:30

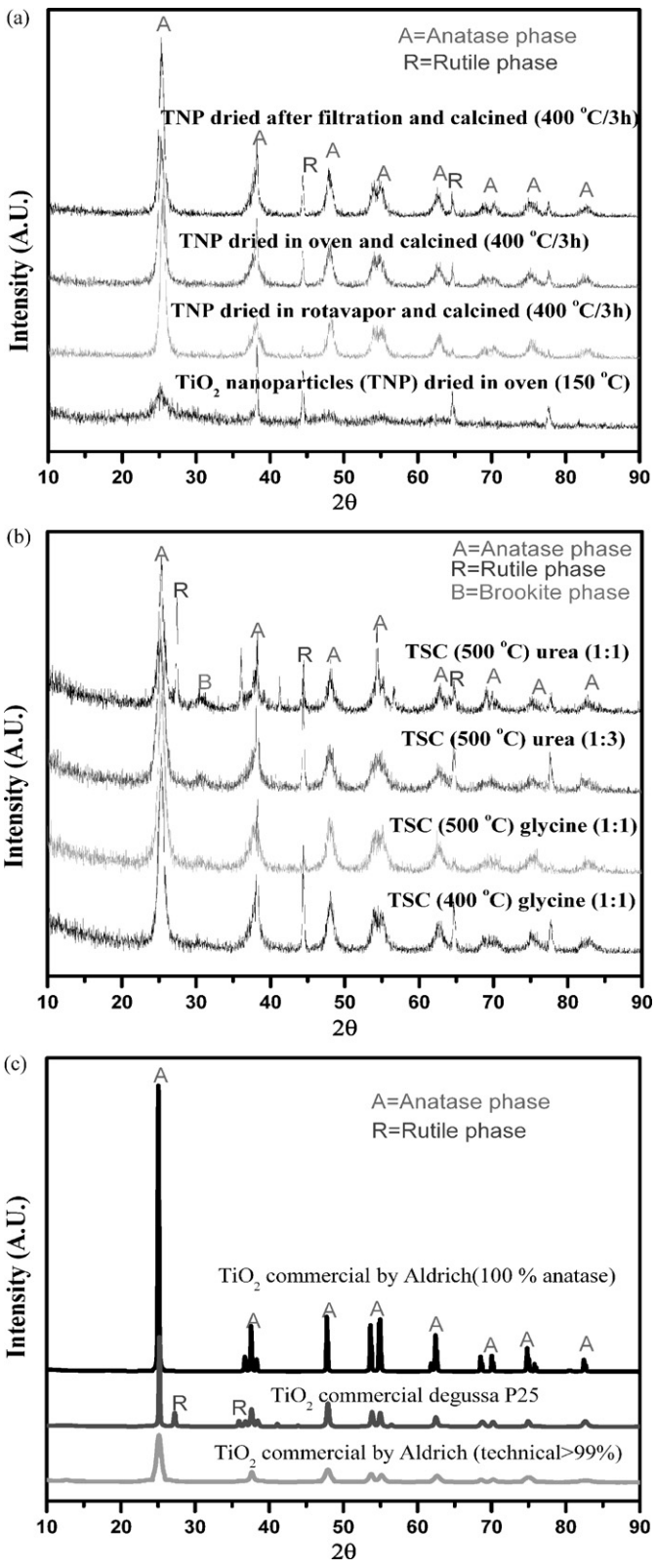

Fig. 3. XRD patterns of (a) TNP, (b) TSC, and (c) different commercial titania.

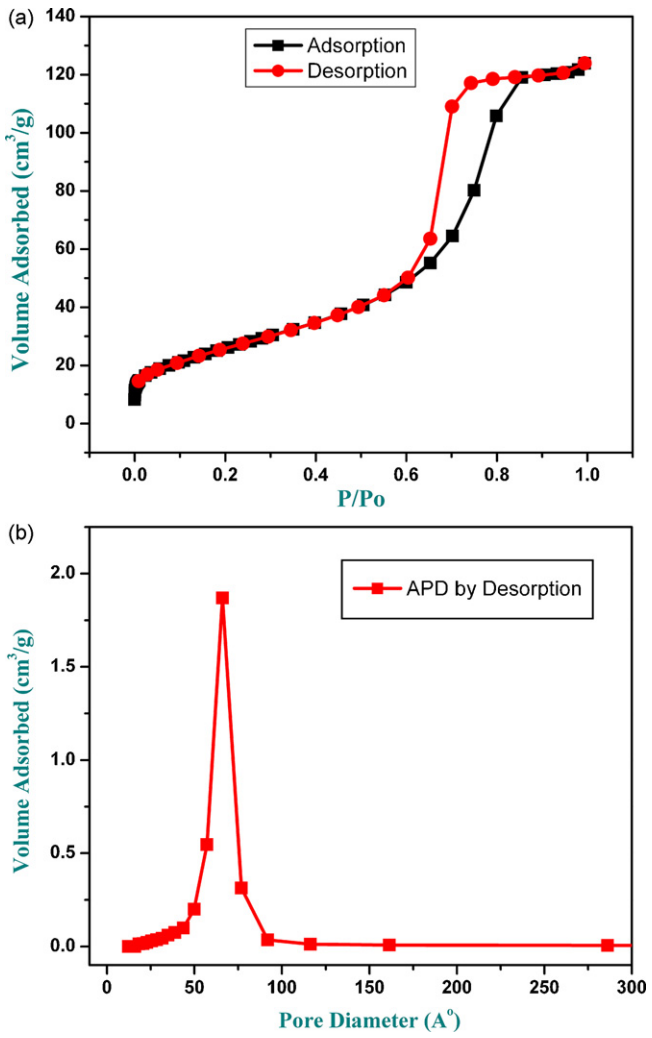

Fig. 4. TNP (rotavapor dried): (a) adsorption/desorption isotherm, (b) average pore diameter.

of anatase being higher than that of rutile [35]. The origin and the method of preparation affect the physico-chemical properties of the specimen. In recent years degussa P25 TiO_2 has set the standard for photoreactivity in environmental VOC applications. Degussa P25 is a non-porous 70:30% (anatase to rutile), having rutile phase but considered even more reactive than pure anatase [6].

Compared to TNP, TSC showed more rutile phase in all the cases shown in Fig. 3(b). However, TSC (glycine, 500 °C, 1:1) and TSC (urea, 500 °C, 1:3) were comparatively better in this category as shown in Table 1. Also, Fig. 3(c) represents the XRD patterns of three different commercial TiO_2 for the comparison. TiO_2 by Aldrich (anatase) showed the pure anatase phase whereas the TiO_2 by Aldrich (technical) has a mixed phase. Degussa P25 also showed mixed anatase and rutile phases.

The effect of the specific surface area of TiO_2 in photocatalysis is always important [6,16]. The primary objective was to synthesize the TNP that have the highest surface area. Table 1 shows that all the TNP samples exhibit higher specific surface area than the TSC as well as all the commercial TiO_2. TNP dried in rotavapor and calcined showed the highest surface area (i.e. 150 m^2/g), in contrast to the degussa P25 (53 m^2/g). It was also reported [6] and shown in Table 1 that surface area of degussa P25 is five times that of Aldrich TiO_2. Therefore comparing all, TNP showed the best available surface area. As shown in Fig. 4(a and b) by adsorption/desorption isotherm and average pore diameter (APD), TNP also have porosity with a pore volume of 0.20 cm^3/g and average pore diameter of 7 nm. This porosity is considered to be the void spaces between the particles in contrast to the non-porous degussa P25. The sample with a porosity and rough surface showed a characteristics of high surface area

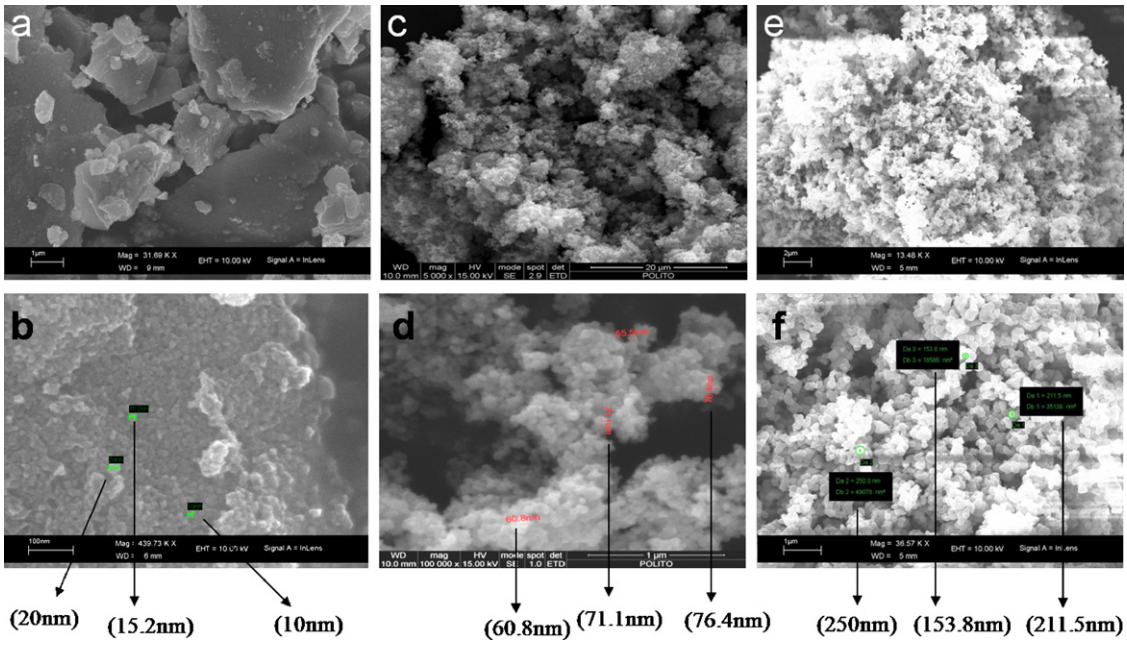

Fig. 5. SEM images of TNP (a and b), degussa P25 (c and d), and TiO_2 commercial by Aldrich (e and f) showing the morphology and particle size difference.

and high adsorptive capacity [16]. Also, the increased surface area of TiO_2 should be helpful to enhance the surface reaction of TiO_2 [36].

FE-SEM was used to analyze the particle size and shape of the calcined TNP and comparison with commercial TiO_2. The SEM images of the calcined TNP showed fine nanoparticles of 10–20 nm range (Fig. 5a and b). Even though the sample was calcined at high temperature of 400 °C for 3 h, the nanoparticles are more in the dispersed phase and very less in the aggregates. On the other hand, degussa P25 showed an aggregates of 60–70 nm nanoparticles (Fig. 5c and d) and Aldrich TiO_2 has much larger size nanoparticles in the range of 150–250 nm (Fig. 5e and f).

EDX a chemical microanalysis technique is used to characterize the elemental composition of the calcined TNP. It demonstrates that the main components are O and Ti with 67 and 32 at.%, respectively confirms the formation of TiO_2 and a small amount of Cl that is actually from HCl added during the synthesis.

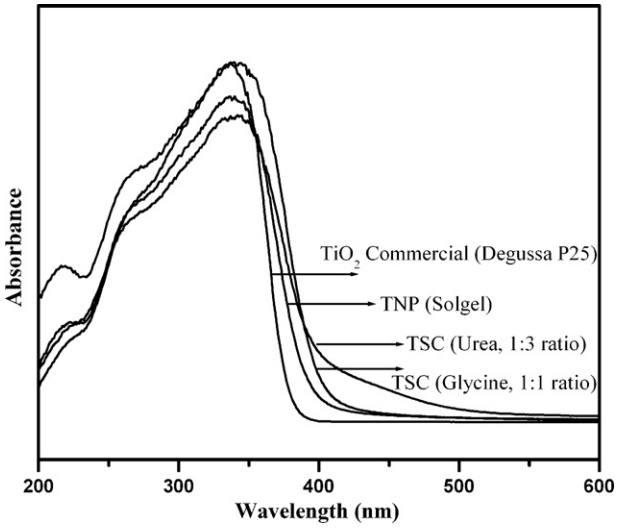

Fig. 6. DR/UV–vis spectra of different titania samples showing the difference in wavelength.

DR/UV–vis directly provides some insight into the interactions of the photocatalytic materials (e.g. TiO_2) with photon energies [9,35,37]. Fig. 6 shows the UV–vis absorption profiles of TNP and TSC calcined at 400 °C/3 h, and compares then with those of commercial TiO_2. It is clear that the absorption spectrum of TNP exhibits an onset of absorption at $\lambda = 391$ nm compared to TSC which shows at $\lambda = 402$, 413 nm, whereas degussa P25 represents at $\lambda = 380$ nm as shown in Fig. 6 and Table 2. The band gap energy of the titania samples was calculated by using this UV–vis DRS spectra with the equation, $E\,(\text{eV}) = hc/\lambda = 1239.95/\lambda$ [37], where E is the band gap energy (eV), h is Planck's constant, c is the velocity of light (m/s) and λ is the wavelength in nm. Table 2 shows the calculated band gap energies and the comparison. The average literature values for the absorption and corresponding band gap energies for bulk anatase TiO_2 is λ_{on} 385 nm and $E = 3.2$ eV [38]. It has also been reported that the increased band gap energy could be attributed to the effect of quantum size [37].

The FT-IR spectra of TNP and TSC calcined at 400 °C/3 h, and degussa P25 is shown in Fig. 7. It is believed that the broad peak at 3400 and the peak at 1650 cm^{-1} correspond to the surface water and hydroxyl groups [39]. Obviously, the calcined TNP has more surface water and hydroxyl groups than the calcined TSC as well as the degussa P25. This can be attributed to the larger surface area of the calcined TNP (Table 1). TNP of large surface area might offer more active sites to adsorb water and generate hydroxyl groups.

3.2. Ethylene photocatalysis

PCO of ethylene over TNP was performed at ambient temperature (Fig. 2) and compared with different TSC and commercial TiO_2

Table 2
Comparison of band gap energies of different TiO_2.

Sample name	Absorption edge wave length, λ (nm)	Band gap energy, E (eV)
TNP (sol–gel)	391	3.17
TSC (glycine)	402	3.08
TSC (urea)	413	3.00
TiO_2 commercial (degussa P25)	380	3.26

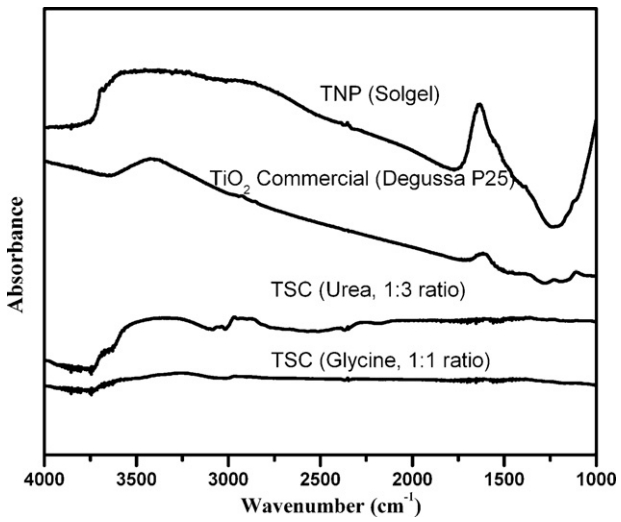

Fig. 7. FT-IR spectra of different titania samples showing the difference in OH groups.

photocatalysts. The important feature of this reaction is the use of air instead of conventional oxygen. In this situation, the required oxygen for the photocatalytic reaction is obtained from the air, leading towards the commercialization step. Fig. 8 shows the percentage conversion of ethylene as a function of time. TNP showed significantly higher conversion than all other samples. Degussa P25 showed comparable results. Even 100% anatase commercial TiO_2 showed very low conversion in this reaction. As it is clear, TSC synthesized with different ways using urea and glycine were also not suitable for this application. TNP was stable active until 6 h of reaction time in contrast to the degussa P25, which starts deactivation at this time. This deactivation of degussa P25 is due to its inferior properties. Moreover, TNP showed higher activity and good stability because of several superior properties which are being discussed in the following paragraphs.

The first superior characteristic of TNP in ethylene photodegradation is that it has main anatase with small rutile phase (Table 1). The photocatalyst derives its activity from the fact that when photons of a certain wavelength hit upon a surface, electrons are

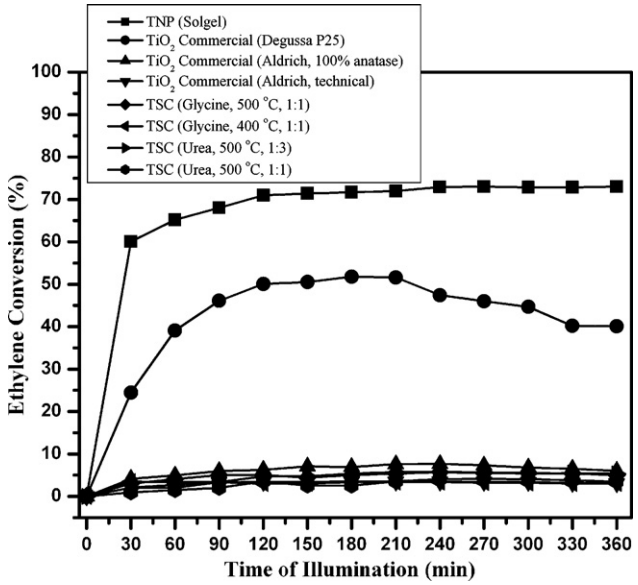

Fig. 8. Ethylene photodegradation over different titania photocatalysts with time of illumination.

promoted from the valence band and transferred to the conductance band [6]. This leaves positive holes in the valence band, which react with the hydroxylated surface to produce $OH^{\bullet}$ radicals which are the most active oxidizing agents. In the absence of suitable electron and hole scavengers, the stored energy is dissipated within a few nanoseconds by recombination. If a suitable scavenger or a surface defect state is available to trap the electron or hole, their recombination is prevented and subsequent redox reaction may occur. In TNP, similar to degussa P25, the conduction band electron of the anatase part jumps to the less positive rutile part, reducing the rate of recombination of electrons and positive holes in the anatase part.

A second favorable feature of TNP in this application is the small size in combination with little porosity (Fig. 5) accompanied by large surface area (Table 1). It is reported that the photochemical characteristics of ultra small particles (i.e. Q-sized particles) has many advantages over comparatively macroparticles such as degussa P25 [40]. These small particles exhibit characteristics between molecular and bulk semiconductor. The high surface area-to-volume ratios lead to improved effectiveness for surface-limited reactions. Porosity between the TNP also make it superior to degussa P25 in ethylene photodegradation. The substances which are readily adsorbed are degraded at faster rate, indicating that the reaction is a surface phenomena [6]. The adsorption of ethylene which is competitive to OH groups on TNP surface might be increased due to this porosity, which causes the higher conversion after reaction.

The third attractive point of TNP is the numerous OH groups on the surface (Fig. 7). It is also noted that the type and amount of surface OH groups and or physisorbed H_2O plays a significant role in the photocatalytic reactions through the formation of OH radicals. The holes can react with water to produce the highly reactive hydroxyl radicals ($OH^{\bullet}$). These holes and the hydroxyl radicals are very powerful oxidants, which oxidize the organic materials [41]. The large surface area of the TNP was one of the most important factors in achieving a high efficiency through higher OH groups adsorbed on the surface of TNP in the PCO of the ethylene.

Another factor which is dominant in TNP (mostly anatase) is its higher bandgap energy (Fig. 6, Table 2) close to degussa P25. It also shows higher band gap energy than TSC due to more anatase phase. Moreover, when the crystallite dimension of a semiconductor particle falls below a critical radius of approximately 10 nm, the charge carriers appear to behave quantum mechanically [36]. As a result of this confinement, the band gap between the valence and conduction bands is enlarged as the particle size of the TiO_2 decreases. Thus, the oxidation potential of the photon generated holes (h^+) and the reducing potential of the electrons (e^-) could increase with increasing bandgap.

4. Conclusions

In this work, novel TNP was successfully synthesized on large scale by sol–gel method using VR with optimized operating parameters and conditions. Characterization comparison was done with the synthesized TSC and commercially purchased TiO_2 using different analysis techniques in detail. TNP showed many superior characteristics to other samples such as: main anatase with small rutile phase, small nanoparticles with little porosity accompanied by a large surface area, high band gap energy, and numerous OH groups.

Photocatalytic application of TNP was tested in the newly fabricated reaction system for the photocatalytic degradation of ethylene and compared with different TSC and commercial TiO_2 in activity. TNP revealed higher photocatalytic conversion of ethylene even than degussa P25, which is the best commercial TiO_2. The enhancement in activity is believed to be due to the all combined

superior features of TNP, mentioned above. The obtained results in this study are very encouraging, showing further way for optimizations and promising applications especially in the photocatalysis of VOCs and many more.

Acknowledgements

This work is supported by Fondazione Cassa di Risparmio di Cuneo. M. Hussain is also thankful to Regione Piemonte and Politechnico di Torino, Italy for the post-doctoral fellowship grant. Prof. Guido Saracco is highly acknowledged for the review of the manuscript.

References

[1] A. Fujishima, K. Honda, Electrochemical photolysis of water at a semiconductor electrode, Nature 238 (1972) 37–38.
[2] B. O'Regan, M. Gratzel, A low-cost, high-efficiency solar cell based on dye-sensitized colloidal TiO_2 films, Nature 353 (1991) 737–740.
[3] R. Blossey, Self-cleaning surfaces-virtual realities, Nat. Mater. 2 (2003) 301–306.
[4] M. Yamagishi, S. Kuriki, P.K. Song, Thin film TiO_2 photocatalyst deposited by reactive magnetron sputtering, Thin Solid Films 442 (2003) 227–231.
[5] U. Bach, D. Corr, D. Lupo, F. Pichot, M. Ryan, Nanomaterials-based electrochromics for paper-quality displays, Adv. Mater. 14 (2002) 845–848.
[6] D.S. Bhatkhande, V.G. Pangarkar, A.A.C.M. Beenackers, Photocatalytic degradation for environmental applications—a review, J. Chem. Technol. Biotechnol. 77 (2001) 102–116.
[7] A. Fujishima, T.N. Rao, D.A. Tryk, Titanium dioxide photocatalysis, J. Photochem. Photobiol. C: Photochem. Rev. 1 (2000) 1–21.
[8] A. Fujishima, X. Zhang, Titanium dioxide photocatalysis: present situation and future approaches, C. R. Chimie 9 (2006) 750–760.
[9] D.B. Hamal, K.J. Klabunde, Synthesis, characterization, and visible light activity of new nanoparticle photocatalysts based on silver, carbon, and sulfur-doped TiO_2, J. Colloids Interf. Sci. 311 (2007) 514–522.
[10] X. Fu, L.A. Clark, W.A. Zeltner, M.A. Anderson, Effects of reaction temperature and water vapor content on the heterogeneous photocatalytic oxidation of ethylene, J. Photochem. Photobiol. A: Chem. 97 (1996) 181–186.
[11] T.W. Tibbitts, K.E. Cushman, X. Fu, M.A. Anderson, R.J. Bula, Factors controlling activity of zirconia–titania for photocatalytic oxidation of ethylene, Adv. Space Res. 22 (1998) 1443–1451.
[12] A. Sirisuk, C.G. Hill Jr., M.A. Anderson, Photocatalytic degradation of ethylene over thin films of titania supported on glass rings, Catal. Today 54 (1999) 159–164.
[13] D.R. Park, J. Zhang, K. Ikeue, H. Yamashita, M. Anpo, Photocatalytic oxidation of ethylene to CO_2 and H_2O on ultrafine powdered TiO_2 photocatalysts in the presence of O_2 and H_2O, J. Catal. 185 (1999) 114–119.
[14] S. Kumar, A.G. Fedorova, J.L. Golea, Photodegradation of ethylene using visible light responsive surfaces prepared from titania nanoparticle slurries, Appl. Catal. B: Environ. 57 (2005) 93–107.
[15] A. Strini, S. Cassese, L. Schiavi, Measurement of benzene, toluene, ethylbenzene and o-xylene gas phase photodegradation by titanium dioxide dispersed in cementitious materials using a mixed flow reactor, Appl. Catal. B: Environ. 61 (2005) 90–97.
[16] L. Zou, Y. Luo, M. Hooper, E. Hu, Removal of VOCs by photocatalysis process using adsorption enhanced TiO_2–SiO_2 catalyst, Chem. Eng. Process. 45 (2006) 959–964.
[17] G.M. Zuo, Z.X. Cheng, H. Chen, G.W. Li, T. Miao, Study on photocatalytic degradation of several volatile organic compounds, J. Hazard. Mater. 128 (2006) 158–163.
[18] D.S. Tsoukleris, T. Maggos, C. Vassilakos, P. Falaras, Photocatalytic degradation of volatile organics on TiO_2 embedded glass spherules, Catal. Today 129 (2007) 96–101.
[19] M. Lamallem, H. El Ayadi, C. Gennequin, R. Cousin, S. Siffert, F. Aissi, A. Aboukais, Effect of the preparation method on Au/Ce–Ti–O catalysts activity for VOCs oxidation, Catal. Today 137 (2008) 367–372.
[20] A.L. Linsebigler, G.Q. Lu, J.T. Yates, Photocatalysis on TiO_2 surfaces—principles, mechanisms, and selected results, Chem. Rev. 95 (1995) 735–758.
[21] S.S. Watson, D. Beydoun, J.A. Scott, R. Amal, The effect of preparation method on the photoactivity of crystalline titanium dioxide particles, Chem. Eng. J. 95 (2003) 213–220.
[22] A. Mills, N. Elliott, G. Hill, D. Fallis, J.R. Durrant, R.L. Willis, Preparation and characterization of novel thick solgel titania film photocatalyst, Photochem. Photobiol. Sci. 2 (2003) 591–596.
[23] M.H. Habibi, H. Vosoghian, Photocatalytic degradation of some organic sulfides as environmental pollutants using titanium dioxide suspension, J. Photochem. Photobiol. A 174 (2005) 45–52.
[24] R.R. Bacsa, J. Kiwi, Effect of rutile phase on the photocatalytic properties of nanocrystalline titania during the degradation of p-coumaric acid, Appl. Catal. B: Environ. 16 (1998) 19–29.
[25] J.M. Warson, A.T. Cooper, J.R.V. Flora, Nanoglued titanium dioxide aerogels for photocatalysis, Environ. Eng. Sci. 22 (2005) 666–675.
[26] M.C. Yan, F. Chen, J.L. Zhang, M. Anpo, Preparation of controllable crystalline titania and study on the photocatalytic properties, J. Phys. Chem. B 109 (2005) 8673–8678.
[27] A. Testino, I.R. Bellobono, V. Buscaglia, C. Canevali, M. D'Arienzo, S. Polizzi, R. Scotti, F. Morazzoni, Optimizing the photocatalytic properties of hydrothermal TiO_2 by the control of phase composition and particle morphology. A systematic approach, J. Am. Chem. Soc. 129 (2007) 3564–3575.
[28] C. Su, B.Y. Hong, C.M. Tseng, Solgel preparation and photocatalysis of titanium dioxide, Catal. Today 96 (2006) 119–126.
[29] S.E. Pratsinis, Synthesis of ceramic powders, Prog. Energy Combust. Sci. 24 (1998) 197–219.
[30] Y.V. Kolen'ko, V.D. Maximov, A.A. Burukhin, V.A. Muhanov, B.R. Churagulov, Synthesis of ZrO_2 and TiO_2 nanocrystalline powders by hydrothermal process, Mater. Sci. Eng. C 23 (2003) 1003.
[31] X.Z. Ding, X.H. Liu, Synthesis and microstructure control of nanocrystalline anatase titania powders via solgel process, Mater. Sci. Eng. A 224 (1997) 210–215.
[32] D.L. Marchisio, F. Omegna, A.A. Barresi, P. Bowen, Effect of mixing and other operating parameters in solgel processes, Ind. Eng. Chem. Res. 47 (2008) 7202–7210.
[33] D.L. Marchisio, F. Omegna, A.A. Barresi, Production of TiO_2 nanoparticles with controlled characteristics by means of a vortex reactor, Chem. Eng. J. 146 (2009) 456–465.
[34] G. Sivalingam, K. Nagaveni, M.S. Hegde, G. Madras, Photocatalytic degradation of various dyes by combustion synthesized nano anatase TiO_2, Appl. Catal. B: Environ. 45 (2003) 23–38.
[35] K. Porkodi, S.D. Arokiamary, Synthesis and spectroscopic characterization of nanostructured anatase titania: a photocatalyst, Mater. Charact. 58 (2007) 495–503.
[36] H.J. Kim, Y.G. Shul, H.S. Han, Photocatalytic properties of silica-supported TiO_2, Top. Catal. 35 (2005) 287–293.
[37] P. Periyat, K.V. Baiju, P. Mukundan, P.K. Pillai, K.G.K. Warrier, High temperature stable mesoporous anatase TiO_2 photocatalyst achieved by silica addition, Appl. Catal. A: Gen. 349 (2008) 13–19.
[38] K. Mogyorosi, I. Dekany, J.H. Fendler, Preparation and characterization of clay mineral intercalated titanium dioxide nanoparticles, Langmuir 19 (2003) 2938–2946.
[39] G. Tian, H. Fu, L. Jing, C. Tian, Synthesis, photocatalytic activity of stable nanocrystalline TiO_2 with high crystallinity and large surface area, J. Hazard. Mater. 161 (2009) 1122–1130.
[40] J. Zhao, X. Yang, Photocatalytic oxidation for indoor air purification: a literature review, Build. Environ. 38 (2003) 645–654.
[41] A. Fujishima, K. Hashimoto, T. Watanabe, TiO_2 Photocatalysis: Fundamentals and Applications, English ed., BKC, Tokyo, 1999.